


Review

# Crystalline Silicon (c-Si)-Based Tunnel Oxide Passivated Contact (TOPCon) Solar Cells: A Review

Hayat Ullah <sup>1</sup>, Stanislaw Czapp <sup>1,\*</sup>, Seweryn Szultka <sup>1</sup>, Hanan Tariq <sup>1</sup>, Usama Bin Qasim <sup>2</sup>  
and Hassan Imran <sup>3</sup>

<sup>1</sup> Faculty of Electrical and Control Engineering, Gdansk University of Technology, Narutowicza 11/12 str., 80-233 Gdansk, Poland

<sup>2</sup> Department of Electrical Engineering, Lahore University of Management Sciences (LUMS), Lahore 54792, Pakistan

<sup>3</sup> Department of Electrical Engineering, GIFT University, Gujranwala 52250, Pakistan

\* Correspondence: stanislaw.czapp@pg.edu.pl

**Abstract:** Contact selectivity is a key parameter for enhancing and improving the power conversion efficiency (PCE) of crystalline silicon (c-Si)-based solar cells. Carrier selective contacts (CSC) are the key technology which has the potential to achieve a higher PCE for c-Si-based solar cells closer to their theoretical efficiency limit. A recent and state-of-the-art approach in this domain is the tunnel oxide passivated contact (TOPCon) approach, which is completely different from the existing classical heterojunction solar cells. The main and core element of this contact is the tunnel oxide, and its main role is to cut back the minority carrier recombination at the interface. A state-of-the-art n-type c-Si-based TOPCon solar cell featuring a passivated rear contact was experimentally analyzed, and the highest PCE record of ~25.7% was achieved. It has a high fill factor (FF) of ~83.3%. These reported results prove that the highest efficiency potential is that of the passivated full area rear contact structures and it is more efficient than that of the partial rear contact (PRC) structures. In this paper, a review is presented which considers the key characteristics of TOPCon solar cells, i.e., minority carrier recombination, contact resistance, and surface passivation. Additionally, practical challenges and key issues related to TOPCon solar cells are also highlighted. Finally, the focus turns to the characteristics of TOPCon solar cells, which offer an improved and better understanding of doping layers and tunnel oxide along with their mutual and combined effect on the overall performance of TOPCon solar cells.

**Keywords:** carrier selective contacts; contact resistance; tunnel oxide passivated contact; renewable energy; surface passivation



**Citation:** Ullah, H.; Czapp, S.; Szultka, S.; Tariq, H.; Qasim, U.B.; Imran, H. Crystalline Silicon (c-Si)-Based Tunnel Oxide Passivated Contact (TOPCon) Solar Cells: A Review. *Energies* **2023**, *16*, 715. <https://doi.org/10.3390/en16020715>

Academic Editors: Konrad Zajkowski, Jacek Paś, Piotr Kisiel and Abdul-Ghani Olabi

Received: 29 November 2022

Revised: 20 December 2022

Accepted: 4 January 2023

Published: 7 January 2023



**Copyright:** © 2023 by the authors. Licensee MDPI, Basel, Switzerland. This article is an open access article distributed under the terms and conditions of the Creative Commons Attribution (CC BY) license (<https://creativecommons.org/licenses/by/4.0/>).

## 1. Introduction

Meeting the world's growing energy demands while simultaneously tackling human-induced global warming has become one of the indisputable challenges that humanity is going to face around the globe in the near future. This requires sustainable energy production from clean and eco-friendly resources. Solar photovoltaic (PV) technology is gaining favorable attention, and this is clearly reflected in the global statistics of the total installed capacity of solar PV modules. Currently, the worldwide cumulative installed capacity of PV modules has already exceeded 700 GW, and its significant increase is expected in the coming years [1,2]. The unique features, such as non-toxicity, abundance, and long-term stability of crystalline silicon (c-Si), have made it a market-dominant technology since the very beginning, with an almost 95% market share [3]. The cost of a c-Si PV module is approximately one-half of the PV system cost and is mainly dominated by material costs, especially by the costs of the Si wafer [4]. On the other hand, the cell manufacturing cost is about one-quarter of the module cost, making it about one-eighth of the complete

PV system's cost [4]. Therefore, besides improved production technology, increasing the efficiency of the cell has significant potential to bring down the system costs even more.

To improve the power conversion efficiency (PCE) of c-Si solar cells closer to its thermodynamic limit of ~29.4% [5], one of the key and fundamental requirements is to improve the photogenerated minority carrier lifetime ( $\tau$ ) by minimizing the recombination losses. As the bulk minority carrier lifetime ( $\tau_{bulk}$ ) in state-of-the-art float-zone (FZ) c-Si wafers has already exceeded 30 ms [6], most of the recombination losses occur at the metal contacts. Therefore, minimizing the contact losses in c-Si solar cells through surface passivation have been an active area of research in recent years. Previously, contact recombination was minimized by introducing a highly doped localized back surface field in a passivated emitter rear locally diffused (PERL) homojunction solar cell. Although PERL solar cells have achieved remarkable efficiency ( $\eta$ ) of ~25% [7], their high fabrication cost (~0.071 \$/W [8]) and low thermal barrier for recombination current carriers at the back has moved researchers towards alternative cost-effective and heterojunction-based approaches.

The Panasonic heterojunction with intrinsic thin layer (HIT) solar cells is the most well-known and traditional example of a heterojunction solar cell. In this solar cell, the c-Si base is sandwiched between thin layers of highly doped amorphous silicon (a-Si) layers [9]. This a-Si/c-Si contact exhibits very low surface passivation, a remarkable open-circuit voltage ( $V_{oc}$ ) of ~750 mV [10], and an outstanding  $\eta$  of ~25.6% [11]. However, the low thermal tolerance to metallization processes [12,13] and parasitic absorption losses due to lower bandgap [14] of a-Si hinder means that further improvement in  $\eta$  for a-Si/c-Si contact-based solar cells is needed. Therefore, researchers are actively searching for alternative surface passivation technologies [15–17] that could maintain low contact resistance while simultaneously minimizing cost per kWh.

One such approach is to replace a-Si with polycrystalline silicon (poly-Si) to avoid stability issues during high-temperature processes (e.g., screen printing) [18,19]. Although poly-Si-based passivating contacts were first introduced almost four decades ago [20–22], the surface defects due to lattice mismatch between poly-Si and c-Si limited their use for solar cells. After that, several research groups also demonstrated that inserting a very thin interfacial oxide ( $\text{SiO}_x$ ) layer between poly-Si and c-Si layers could enhance  $V_{oc}$  up to 720 mV [23–26]. Although a remarkable  $V_{oc}$  has been demonstrated for these contacts, wide interest and attention were gained in 2014 when Feldmann et al. demonstrated  $\eta$  of ~23% for these contacts on the *n*-type c-Si substrate [27]. These passivating contacts based on poly-Si and ultrathin  $\text{SiO}_x$  layers were termed tunnel oxide passivating contacts and known by the abbreviation TOPCon [27].

One of the major benefits of TOPCon is that, in these structures, the c-Si wafer does not come into direct contact with the metal, rather it is separated by a stack of poly-Si and  $\text{SiO}_x$  layers and hence exhibits a reduced Fermi level pinning (FLP) effect [28]. Another major advantage is that the  $\text{SiO}_x$  layer provides excellent carrier selectivity by allowing drift currents of only one type of carrier through quantum mechanical tunneling and thus suppressing the minority carrier recombination at the contact [29]. Several research groups [30–32] have demonstrated that the stack of highly doped poly-Si and ultrathin  $\text{SiO}_x$  ( $\leq 2$  nm) layers provides excellent surface passivation, reduced parasitic absorption losses, low dark current density ( $J_0 < 5$  fA/cm<sup>2</sup>), and low contact resistivity ( $\rho_c < 1$  m $\Omega$ cm<sup>2</sup>) [33–35]. The lab-scale TOPCon solar cell developed by Fraunhofer ISE has demonstrated a remarkable efficiency ( $\eta$ ) of 25.7% [36,37] whereas TOPCon-based solar cells on a large area c-Si wafer developed by LONGi has demonstrated  $\eta$  of 25.1% [38].

The International Technology Roadmap for Photovoltaic (ITRPV) 2021 report confirmed that solar cells with diffused and passivated p-n junctions and passivated rear sides, which mainly include PERC/PERL/PERT/TOPCon (PERC—Passivated Emitter and Rear Cell; PERT—Passivated Emitter Rear Totally Diffused) have completely dominated the solar photovoltaics market [39]. It also claimed in the report that back surface field (BSF) will only be produced on cost-efficient multi-crystalline silicon wafers, and it has a possibility to vanish after 2025. As shown in Figure 1, it is clear that in 2020, the market shares

of PERC/PERL/PERT/TOPCon solar cells slightly exceeded the Information Handling Services (IHS) market assumptions. From Figure 2, it is clear that the TOPCon solar cells will gradually capture 50% of the market shares within the next decade compared to the current market share of ~6%, which obviously shows its dominance in the solar photovoltaic industry and market. Additionally, it is shown that there was a gradual increase in the market shares of Si-heterojunction (HJT) and HIT solar cells of about 10% in 2025 and 18% in 2031, respectively.

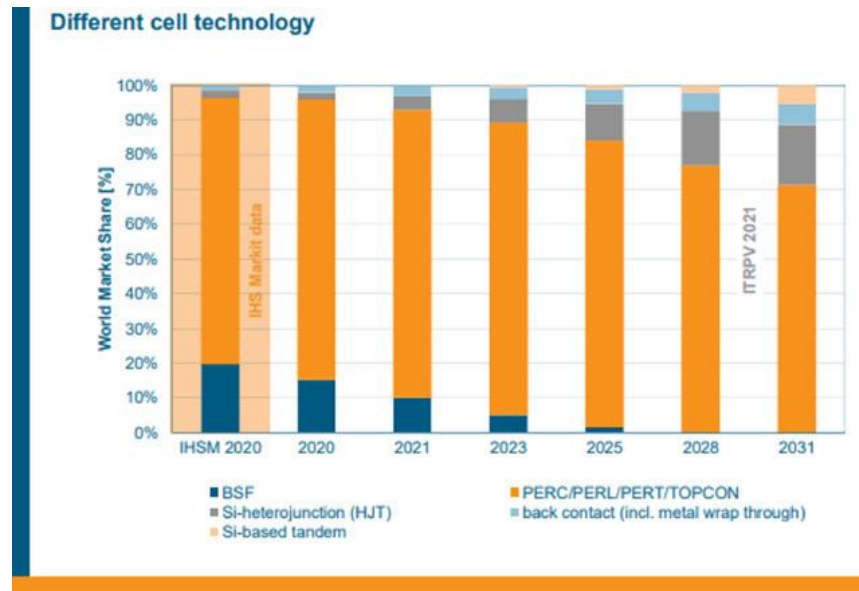


Figure 1. Worldwide market share for different technologies-based solar cells [40]; all acronyms are defined in the main text.

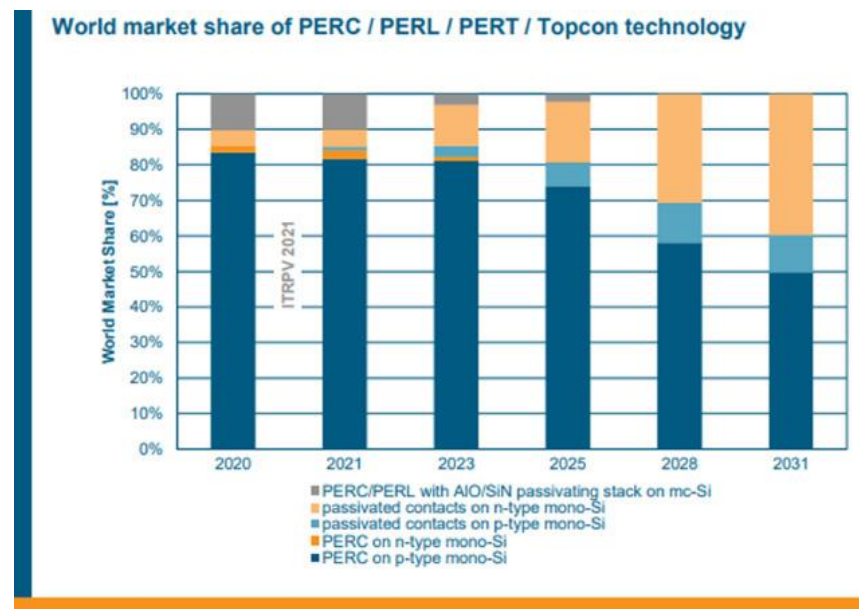


Figure 2. Worldwide market share of TOPCon and PERC/PERL/PERT solar cells [40]; all acronyms are defined in the main text.

Again, Figure 1 clearly endorses that the double-sided contact cell concept dominates all other technologies in terms of market shares. As shown in Figure 1, the rear-side contact cells are predicted to increase in terms of market shares from 2% in 2020 to almost 5% in 2031. In addition to this, the HIT/HJT or Interdigitated Back Contact (IBC) solar cells have

smaller market shares in the current scenario, and it is due to factors such as high cost, complex fabrication, and processing techniques that the need for significant modification of cell processing technologies and low throughput is expected [40].

The further part of this paper presents the structure, parameters, and properties of the TOPCon solar cell.

## 2. Structure and Electrostatics of TOPCon Solar Cell

According to ITRPV, high efficiency and state-of-the-art PERC, along with its variants (e.g., PERL), dominated the PV market with a ~80% share in 2020 [39]. Opportunities exist for those technologies that promise lower production costs with minimal changes to the existing production lines for PERC solar cells. As the fabrication of TOPCon technology cells just adds a few steps in the existing manufacturing units of PERC cells [4,41], therefore it is fundamentally compatible to replace PERC solar cells.

The two-dimensional (2-D) schematic diagram of the TOPCon solar cell is shown in Figure 3. It is produced with c-Si, which has a  $p$ - $n$  junction with a heavily  $p$ -doped emitter on the front side and an  $n$ -type substrate [41].

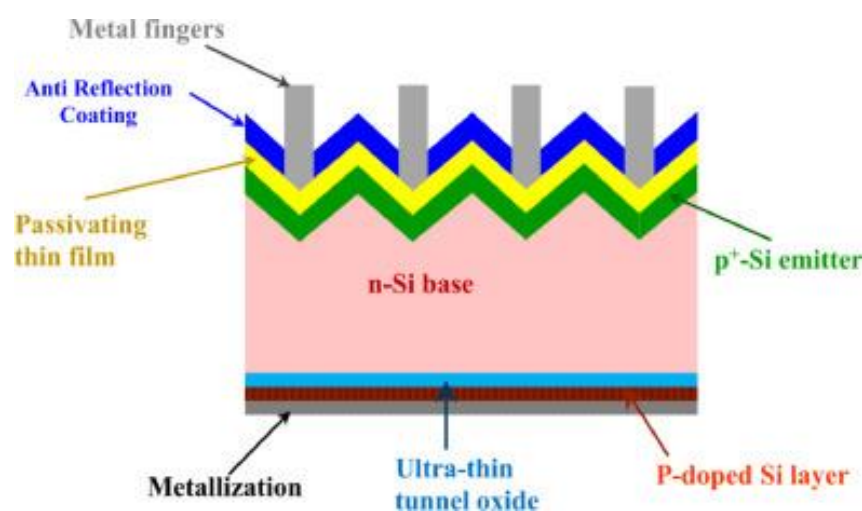


**Figure 3.** Two-dimensional schematic of an n-type c-Si-based TOPCon solar cell [40].

At the front surface, the  $\text{SiN}_x$  layer is used as an anti-reflecting coating, whereas a thin layer of aluminum oxide ( $\text{Al}_2\text{O}_3$ ) is used for the passivating layer, reducing the surface recombination velocity below 50 cm/s [42,43]. At the back, an ultrathin ( $\leq 2$  nm) tunneling layer of  $\text{SiO}_2$  is used as an electron transport layer, whereas a thin layer of the heavily  $n$ -doped poly-Si layer is used to provide an Ohmic contact at the back and electric field for the photogenerated electrons to tunnel through the  $\text{SiO}_2$  layer [29].

## 3. Configurations of the TOPCon in c-Si-Based Solar Cells

There are two different types of configurations possible for the TOPCon, which can be used as a rear contact in c-Si-based solar cells. These are the following:

1. n-TOPCon rear contact for n-type c-Si solar cell
2. p-TOPCon rear contact for p-type c-Si solar cell.

### 3.1. n-TOPCon Rear Contact for n-Type c-Si Solar Cell

The PV cell structure of the n-TOPCon, which is used as a rear contact for the n-type c-Si-based solar cells [43], is shown in Figure 3. The structure contains tunnel oxide, which is developed and grown in nitric acid [44], with a layer of P-doped silicon. Afterward, the a-Si layer was deposited, and the contact was further strengthened and hardened through an annealing process at a very high temperature, which ranges between 800 °C and 900 °C. After annealing, this structure was exposed to hydrogen passivation for a duration of about

30 min at a temperature of 400 °C [45]. The n-type TOPCon structure is used as a rare contact in the n-type c-Si-based solar cell, which has achieved the highest efficiency of up to 25.7% at the cell level [11]. Additionally, it provides extremely excellent and outstanding surface passivation at the Schottky interface. Moreover, it also reduces the contact resistance at the interface [46,47].

### 3.2. *p*-TOPCon Rear Contact for *p*-Type c-Si Solar Cell

The cell structure of the *p*-TOPCon used as a rear contact for the *p*-type c-Si-based solar cells consists of a full-area TOPCon emitter at the rear contact with an oxide layer [40,48], as shown in Figure 4. This structure is designed by using the method of a wet-chemically grown silicon oxide (SiO<sub>x</sub>) layer, which is an extremely thin layer. Moreover, it is also covered with a thick layer of phosphorous-doped silicon carbide (SiC). The thickness of this layer is equal to 15 nm, and it is deposited by using the process of plasma-enhanced chemical vapor deposition (PECVD), which was further strengthened and hardened through an annealing process in a tube furnace at a high temperature of up to 800 °C [43]. The *p*-type TOPCon structure was used as a rare contact in the *p*-type c-Si-based solar cell and achieved the very best efficiency at the cell level of ~24.3% [48]. The conversion efficiency of the *p*-TOPCon used as a rare contact is lower than that of the n-TOPCon. The main reason for this reduction is a slightly increased or magnified series resistance at the interface compared to that of n-TOPCon as a rear contact.

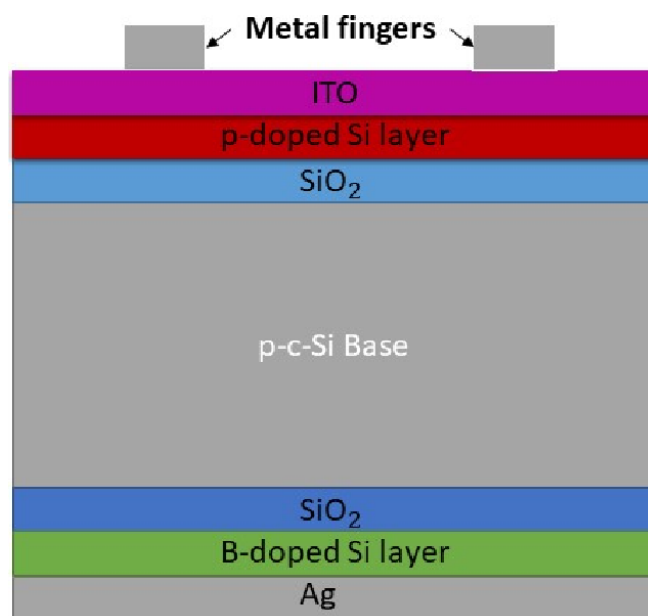


**Figure 4.** Schematic diagram of *p*-type c-Si TOPCon solar cell [40].

## 4. Fabrication of TOPCon Solar Cell

The TOPCon solar cell is mostly produced on a phosphorus-doped c-Si wafer obtained through the Czochralski (CZ) method [49], as shown in Figure 5. This is because low amounts of oxygen are required for phosphorus-doped wafers with  $\rho \approx 0.5 \Omega\text{cm}$  [50]. The steps involved in the assembly for the fabrication of the TOPCon cell are presented in Figure 5 in the form of boxes. First of all, the c-Si wafer is double-sided textured with irregular pyramids using a potassium hydroxide (KOH) solution, which is described by the “Texture” box as shown in Figure 5. After standard RCA (Radio Corporation of America) cleaning, the wafer is kept in a boron diffusion furnace to form the boron-doped (or *p*-type) emitter using a boron tribromide (BBr<sub>3</sub>) source. Then, by using a hydrofluoric acid and nitric acid (HF/HNO<sub>3</sub>) solution, the bottom boron-doped emitter is removed through a single-side etching process. In the next step, the wafer is cleaned using chemicals, and then a stack of passivation layers consisting of ultrathin SiO<sub>x</sub> and intrinsic poly-Si layers is

developed, which is described by thermal  $\text{SiO}_x$ +i-poly and SSE+ cleaning tabs, as shown in Figure 5. The  $\text{SiO}_x$  layer is thermally grown, whereas the poly-Si layer is developed in a low-pressure chemical vapor deposition (LPCVD) system. Then, intrinsic poly-Si is *n*-doped in a phosphoryl chloride ( $\text{POCl}_3$ ) diffusion furnace. The front side of the wafer is cleaned from poly-Si through another single-side etching process. The wafer is again cleaned through the RCA process, and then an anti-reflection and passivation layer is formed in front of the boron-doped emitter. A layer of  $\text{SiN}_x$  using PECVD is formed on the back to protect  $\text{SiO}_x$  and the poly-Si passivation stack. In the last step, an H-shaped metal contact with nine busbars is formed on both sides using screen printing and high-temperature ( $\sim 760^\circ\text{C}$ ) firing methods in order to provide metal contacts [48]. After fabrication, the current voltage ( $J - V$ ) and other valuable characteristics are measured under the standard solar spectrum of AM1.5G ( $1000\text{ W/m}^2$ ) using some suitable flasher instruments.

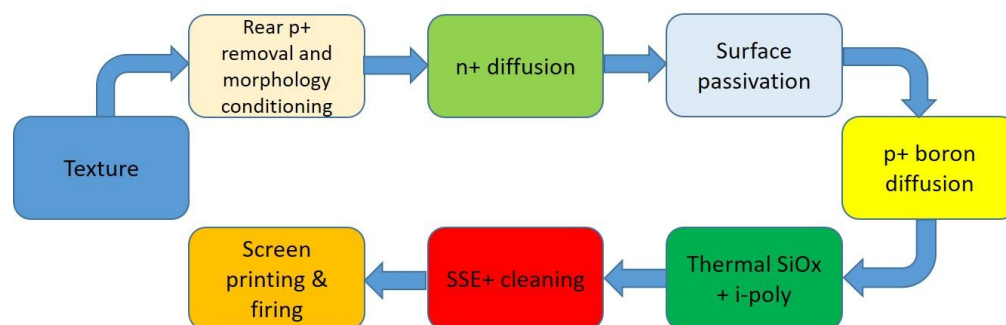


**Figure 5.** Process flow of TOPCon solar cells.

## 5. Discussion

The c-Si-based TOPCon solar cells are under extensive research throughout the world with the main aim of achieving the maximum possible energy conversion efficiencies near the theoretical limit of c-Si-based solar cells. TOPCon solar cells were first highlighted by the Fraunhofer ISE research group in 2013 with an efficiency of  $\sim 21.8\%$ . However, researchers noted that this novel structure had the potential to achieve maximum efficiency close to the theoretical efficiency limit by further exploration. Various research groups and institutes carried out continuous research in this domain and achieved the highest conversion efficiency of  $\sim 25.7\%$  (Figure 6) on a cellular level for single junction c-Si-based solar cells with a  $V_{oc}$  of 725 mV,  $J_{sc}$  of  $42.5\text{ mA/cm}^2$ , and FF of 83.3%, which is very close to the theoretical efficiency limit determined by Shockley-Queisser. Additionally, larger solar cells and modules have been made with a higher power output than the existing PERC solar modules, which currently dominate the market. In parallel to this, a number of industries have made bifacial TOPCon solar cells and modules, with the highest front-side conversion efficiency reaching 25.4%. A comparison is shown in Table 1 among the available single-junction structures of c-Si-based solar cells.

Among all these available technologies presented in Table 1, the TOPCon solar cell has the highest efficiency except the Heterojunction Back Contact (HBC) and p-type poly-Si on oxide (POLO-IBC), which is 0.4% and 1% higher than TOPCon solar cells [16,51,52]. The results (plots) in Figure 6 for the TOPCon show that the oxide layer at the contact provides better passivation in TOPCon solar cells. Therefore, the recombination losses at the contact are significantly reduced compared to standard technology.

In this area of research, still, there are alternatives available for researchers to explore new and state-of-the-art materials for constructing nearly ideal metal oxides to provide the best surface passivation at the semiconductor (c-Si)/metal (Schottky) interface to minimize and reduce contact resistance. As a result, it will reduce the minority carrier recombination at the interface and enhance the majority carrier flow, which improves and enhances the overall performance.

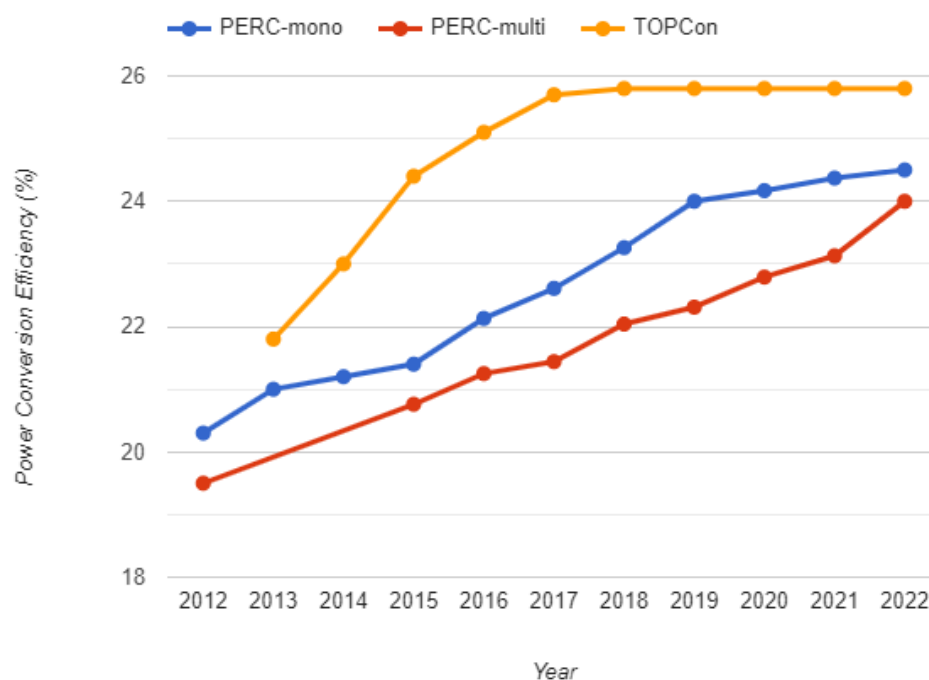


**Figure 6.** Comparison of power conversion efficiency between PERC-mono-, PERC-multi-, and TOPCon-based solar cells with c-Si as a base material. Data from [37].

**Table 1.** Efficiency comparison of various c-Si based solar cell technologies. Data from [37].

Single Junction Structure	Cell Efficiency (%)	Cell Area (cm <sup>2</sup> )	Year	Group/Institute
p-type PERC	25.0	4	1998	UNSW
IBC	25.2	153.5	2012	SunPower
HIT Rear Junction	25.6	143.7	2014	Panasonic
TOPCon	25.7	4	2017	Fraunhofer
HBC	26.7	79	2017	Kaneka
p-type POLO-IBC	26.1	3.98	2018	ISFH

## 6. Conclusions

In this paper, we present a concise review of the c-Si-based TOPCon solar cells. This is a novel research topic in the area of solar cells, which has the potential of achieving maximum energy conversion efficiency for c-Si-based solar cells that are approximately equal to their theoretical limit by using the TOPCon configuration. Until now, the highest possible efficiency achieved for c-Si-based TOPCon at the cell level is up to 25.7% by the Fraunhofer ISE research institute in Germany. Various research groups and institutes are working in this area and exploring it further to improve the overall efficiency of TOPCon solar cells. In this research area, there are still many possibilities for researchers to discover new and state-of-the-art materials for making nearly ideal metal oxides. This ideal metal oxide will be able to provide the best surface passivation at the semiconductor (c-Si)/metal (Schottky) interface by minimizing contact resistance. Hence, it also reduces the minority carrier recombination at the interface along with enhancing the majority carriers flow to improve and enhance the conversion efficiency of the TOPCon solar cells in an economical way.

However, there are still some areas that need more focus and attention to further improve the efficiency of TOPCon solar cells. It mainly includes the fabrication and manufacturing of thin wafer (c-Si)-based TOPCon solar cells, analyzing the impact of using a metal oxide-based carrier selective contact layer instead of a doped poly-Si layer, improving the reflection of evanescent light from the back of the cell through a suitable

interfacial layer between the doped poly-Si layer and rear side silver metallic contact, and the simplification of the manufacturing process for TOPCon-upgraded PERC solar cells.

**Author Contributions:** Conceptualization, H.U. and H.I.; methodology, H.U., U.B.Q. and H.I.; validation, H.U., H.I. and S.C.; formal analysis, H.U., U.B.Q. and H.I.; investigation, H.U., H.I. and S.C.; resources, H.U., H.I., S.S. and S.C.; data curation, H.U. and H.I.; writing—original draft preparation, H.U.; writing—review and editing, H.I., S.S. and S.C.; visualization, H.U., H.T. and H.I.; supervision, S.S. and S.C.; project administration, S.S. and S.C. All authors have read and agreed to the published version of the manuscript.

**Funding:** This research received no external funding.

**Institutional Review Board Statement:** Not applicable.

**Informed Consent Statement:** Not applicable.

**Data Availability Statement:** The data are contained within the article.

**Conflicts of Interest:** The authors declare no conflict of interest.

## References

1. International Energy Agency (IEA) Home Page. Available online: [https://iea.blob.core.windows.net/assets/1a24f1fe-c971-4c25-964a-57d0f31eb97b/Renewables\\_2020-PDF.pdf](https://iea.blob.core.windows.net/assets/1a24f1fe-c971-4c25-964a-57d0f31eb97b/Renewables_2020-PDF.pdf) (accessed on 26 November 2022).
2. The International Renewable Energy Agency (IRENA) Home Page. Available online: [https://www.irena.org/-/media/Files/IRENA/Agency/Publication/2021/Apr/IRENA\\_-RE\\_Capacity\\_Highlights\\_2021.pdf?la=en&hash=1E133689564BC40C2392E85026F71A0D7A9C0B91](https://www.irena.org/-/media/Files/IRENA/Agency/Publication/2021/Apr/IRENA_-RE_Capacity_Highlights_2021.pdf?la=en&hash=1E133689564BC40C2392E85026F71A0D7A9C0B91) (accessed on 23 November 2022).
3. Fraunhofer Institute for Solar Energy Systems (ISE) Home Page. Available online: <https://www.ise.fraunhofer.de/content/dam/ise/de/documents/publications/studies/Photovoltaics-Report.pdf> (accessed on 23 November 2022).
4. Blakers, A. Development of the PERC solar cell. *IEEE J. Photovolt.* **2019**, *9*, 629–635. [CrossRef]
5. Richter, A.; Hermle, M.; Glunz, S.W. Reassessment of the limiting efficiency for crystalline silicon solar cells. *IEEE J. Photovolt.* **2013**, *3*, 1184–1191. [CrossRef]
6. Cuevas, A.; Macdonald, D.H. Measuring and interpreting the lifetime of silicon wafers. *Sol. Energy* **2004**, *76*, 255–262. [CrossRef]
7. Green, M.A. The Passivated Emitter and Rear Cell (PERC): From conception to mass production. *Sol. Energy Mater. Sol. Cells.* **2015**, *143*, 190–197. [CrossRef]
8. Kumar, A.; Bieri, M.; Reindl, T.; Aberle, A.G. Economic viability analysis of silicon solar cell manufacturing: Al-BSF versus PERC. *Energy Procedia* **2017**, *130*, 43–49. [CrossRef]
9. Taguchi, M.; Terakawa, A.; Maruyama, E.; Tanaka, M. Obtaining a higher Voc in HIT cells. *Prog. Photovolt. Res. Appl.* **2005**, *13*, 481–488. [CrossRef]
10. Taguchi, M.; Yano, A.; Tohoda, S.; Matsuyama, K.; Nakamura, Y.; Nishiwaki, T.; Fujita, K.; Maruyama, E. 24.7% record efficiency HIT solar cell on thin silicon wafer. *IEEE J. Photovolt.* **2013**, *4*, 96–99. [CrossRef]
11. Masuko, K.; Shigematsu, M.; Hashiguchi, T.; Fujishima, D.; Kai, M.; Yoshimura, N.; Yamaguchi, T.; Ichihashi, Y.; Mishima, T.; Matsubara, N.; et al. Achievement of more than 25% conversion efficiency with crystalline silicon heterojunction solar cell. *IEEE J. Photovolt.* **2014**, *4*, 1433–1435. [CrossRef]
12. Baert, K.A.; Roggen, J.; Nijs, J.F.; Mertens, R.P. Amorphous-silicon solar cells with screen-printed metallization. *IEEE Trans. Electron. Devices* **1990**, *37*, 702–707. [CrossRef]
13. Melskens, J.; Smets, A.H.M.; Schouten, M.; Eijt, S.W.H.; Schut, H.; Zeman, M. New insights in the nanostructure and defect states of hydrogenated amorphous silicon obtained by annealing. *IEEE J. Photovolt.* **2013**, *3*, 65–71. [CrossRef]
14. Holman, Z.C.; Descoeudres, A.; Barraud, L.; Fernandez, F.Z.; Seif, J.P.; De Wolf, S.; Ballif, C. Current losses at the front of silicon heterojunction solar cells. *IEEE J. Photovolt.* **2012**, *2*, 7–15. [CrossRef]
15. Imran, H.; Abdolkader, T.M.; Butt, N.Z. Carrier-selective NiO/Si and TiO<sub>2</sub>/Si contacts for silicon heterojunction solar cells. *IEEE Trans. Electron. Devices* **2016**, *63*, 3584–3590. [CrossRef]
16. Ullah, H.; Imran, H.; Butt, N.Z. Modeling of TiO<sub>2</sub>-Based Electron-Selective Contacts for Crystalline Silicon Solar Cells. *IEEE Trans. Electron. Devices* **2018**, *65*, 4421–4428. [CrossRef]
17. Nagamatsu, K.A.; Avasthi, S.; Sahasrabudhe, G.; Man, G.; Jhaveri, J.; Berg, A.H.; Schwartz, J.; Kahn, A.; Wagner, S.; Sturm, J.C. Titanium dioxide/silicon hole-blocking selective contact to enable double-heterojunction crystalline silicon-based solar cell. *Appl. Phys. Lett.* **2015**, *106*, 123906. [CrossRef]
18. Stodolny, M.K.; Lenes, M.; Wu, Y.; Janssen, G.; Romijn, I.G.; Luchies, J.; Geerligs, L.J. n-Type polysilicon passivating contact for industrial bifacial n-type solar cells. *Sol. Energy Mater. Sol. Cells* **2016**, *158*, 24–28. [CrossRef]
19. Tao, Y.; Upadhyaya, V.; Chen, C.W.; Payne, A.; Chang, E.L.; Upadhyaya, A.; Rohatgi, A. Large area tunnel oxide passivated rear contact n-type Si solar cells with 21.2% efficiency. *Prog. Photovolt. Res. Appl.* **2016**, *24*, 830–835. [CrossRef]
20. Swanson, R.M. A proposed thermophotovoltaic solar energy conversion system. *Proc. IEEE* **1979**, *67*, 446–447. [CrossRef]



21. Green, M.A.; Blakers, A.W. Advantages of metal-insulator-semiconductor structures for silicon solar cells. *Sol. Cells* **1983**, *8*, 3–16. [CrossRef]
22. Inoue, N.; Miyakawa, T.; Wilmsen, C.W. An analysis of EBIC Response of ITO/poly-Si Solar cells. *JJAP* **1981**, *20*, 11–15. [CrossRef]
23. Yablonovitch, E.; Gmitter, T.; Swanson, R.M.; Kwark, Y.H. A 720 mV open circuit voltage SiO<sub>x</sub>: C-Si: SiO<sub>x</sub> double heterostructure solar cell. *Appl. Phys. Lett.* **1985**, *47*, 1211–1213. [CrossRef]
24. Tarr, N.G. A polysilicon emitter solar cell. *IEEE Electron. Device Lett.* **1985**, *6*, 655–658. [CrossRef]
25. Lindholm, F.A.; Neugroschel, A.; Arienzo, M.; Iles, P.A. Heavily doped polysilicon-contact solar cells. *IEEE Electron. Device Lett.* **1985**, *6*, 363–365. [CrossRef]
26. Kwark, Y.H.; Swanson, R.M. N-type SIPOS and poly-silicon emitters. *Solid-State Electron.* **1987**, *30*, 1121–1125. [CrossRef]
27. Feldmann, F.; Bivour, M.; Reichel, C.; Hermle, M.; Glunz, S.W. Passivated rear contacts for high-efficiency n-type Si solar cells providing high interface passivation quality and excellent transport characteristics. *Sol. Energy Mater. Sol. Cells* **2014**, *120*, 270–274. [CrossRef]
28. Robertson, J. Band offsets of wide-band-gap oxides and implications for future electronic devices. *J. Vac. Sci. Technol. B* **2000**, *18*, 1785–1791. [CrossRef]
29. Younas, R.; Imran, H.; Shah, S.I.; Abdolkader, T.M.; Butt, N.Z. Computational modeling of polycrystalline silicon on oxide passivating contact for silicon solar cells. *IEEE Trans. Electron. Devices* **2019**, *66*, 1819–1826. [CrossRef]
30. Hollemann, C.; Haase, F.; Schafer, S.; Krügener, J.; Brendel, R.; Peibst, R. 26.1%- efficient POLO-IBC cells: Quantification of electrical and optical loss mechanisms. *Prog. Photovolt. Res. Appl.* **2019**, *27*, 950–958. [CrossRef]
31. Rohatgi, A.; Rounsaville, B.; Ok, Y.W.; Tam, A.M.; Zimbardi, F.; Upadhyaya, A.D.; Tao, Y.; Madani, K.; Richter, A.; Benick, J.; et al. Fabrication and modeling of high-efficiency front junction n-type silicon solar cells with tunnel oxide passivating back contact. *IEEE J. Photovolt.* **2017**, *7*, 1236–1243. [CrossRef]
32. Peibst, R.; Römer, U.; Larionova, Y.; Rienäcker, M.; Merkle, A.; Folchert, N.; Reiter, S.; Turcu, M.; Min, B.; Krügener, J.; et al. Working principle of carrier selective poly-Si/c-Si junctions: Is tunnelling the whole story? *Sol. Energy Mater. Sol. Cells* **2016**, *158*, 60–67. [CrossRef]
33. Römer, U. Polycrystalline Silicon/Monocrystalline Silicon Junctions and Their Application as Passivated Contacts for Si Solar Cells. Doctoral Thesis, Gottfried Wilhelm Leibniz Universität Hannover, Hannover, Germany, 2016. Available online: <https://www.repo.uni-hannover.de/handle/123456789/8614?locale-attribute=en> (accessed on 22 November 2022).
34. Römer, U.; Peibst, R.; Ohrdes, T.; Lim, B.; Krügener, J.; Wietler, T.; Brendel, R. Ion implantation for poly-Si passivated back-junction back-contacted solar cells. *IEEE J. Photovolt.* **2015**, *5*, 507–514. [CrossRef]
35. Rienäcker, M.; Bossmeyer, M.; Merkle, A.; Römer, U.; Haase, F.; Krügener, J.; Brendel, R.; Peibst, R. Junction resistivity of carrier-selective polysilicon on oxide junctions and its impact on solar cell performance. *IEEE J. Photovolt.* **2017**, *7*, 11–18. [CrossRef]
36. Richter, A.; Benick, J.; Feldmann, F.; Fell, A.; Hermle, M.; Glunz, S.W. n-Type Si solar cells with passivating electron contact: Identifying sources for efficiency limitations by wafer thickness and resistivity variation. *Sol. Energy Mater. Sol. Cells* **2017**, *173*, 96–105. [CrossRef]
37. Green, M.A.; Dunlop, E.D.; Hohl-Ebinger, J.; Yoshita, M.; Kopidakis, N.; Hao, X. Solar cell efficiency tables (Version 58). *Prog. Photovolt. Res. Appl.* **2021**, *29*, 657–667. [CrossRef]
38. Shaw, V. Pv Magazine Home Page. Available online: <https://www.pv-magazine.com/2021/05/03/longi-sets-topcon-cell-record-of-25-09/> (accessed on 23 November 2022).
39. International Technology Roadmap for Photovoltaic (ITRPV) Home Page. Available online: [https://itrvp.vdma.org/documents/27094228/67038244/2021-04-29%20PR%20VDMA%20PV%20ITRPV%202021%20EN\\_1619690887765.pdf/644380bd-85a3-99d9-e25f-c4ccc6556e64](https://itrvp.vdma.org/documents/27094228/67038244/2021-04-29%20PR%20VDMA%20PV%20ITRPV%202021%20EN_1619690887765.pdf/644380bd-85a3-99d9-e25f-c4ccc6556e64) (accessed on 23 November 2022).
40. Ghosh, D.K.; Bose, S.; Das, G.; Acharyya, S.; Nandi, A.; Mukhopadhyay, S.; Sengupta, A. Fundamentals, present status and future perspective of TOPCon solar cells: A comprehensive review. *Surf. Interfaces* **2022**, *30*, 101917. [CrossRef]
41. Wilson, G.M.; Al-Jassim, M.; Metzger, W.K.; Glunz, S.W.; Verlinden, P.; Xiong, G.; Mansfield, L.M.; Stanbery, B.J.; Zhu, K.; Yanfa, Y.; et al. The 2020 photovoltaic technologies roadmap. *J. Phys. D.* **2020**, *53*. [CrossRef]
42. Kafle, B.; Goraya, B.S.; Mack, S.; Feldmann, F.; Nold, S.; Rentsch, J. TOPCon–Technology options for cost efficient industrial manufacturing. *Sol. Energy Mater. Sol. Cells* **2021**, *227*, 111100. [CrossRef]
43. Yang, X.; Weber, K. N-type silicon solar cells featuring an electron-selective TiO<sub>2</sub> contact. In Proceedings of the 2015 IEEE 42nd Photovoltaic Specialist Conference (PVSC 2015), New Orleans, LA, USA, 14–19 June 2015; pp. 1–4.
44. Yang, X.; Bi, Q.; Ali, H.; Davis, K.; Schoenfeld, W.V.; Weber, K. High-performance TiO<sub>2</sub>-based electron-selective contacts for crystalline silicon solar cells. *Adv. Mater.* **2016**, *28*, 5891–5897. [CrossRef]
45. Macco, B.; Vos, M.F.; Thissen, N.F.; Bol, A.A.; Kessels, W.M. Low-temperature atomic layer deposition of MoO<sub>x</sub> for silicon heterojunction solar cells. *Phys. Status Solidi RRL Rapid Res. Lett.* **2015**, *9*, 393–396. [CrossRef]
46. Bivour, M.; Temmler, J.; Steinkemper, H.; Hermle, M. Molybdenum and tungsten oxide: High work function wide band gap contact materials for hole selective contacts of silicon solar cells. *Sol. Energy Mater. Sol. Cells* **2015**, *142*, 34–41. [CrossRef]
47. Feldmann, F.; Bivour, M.; Reichel, C.; Hermle, M.; Glunz, S.W. A passivated rear contact for high-efficiency n-type silicon solar cells enabling high Voc and FF > 82%. In Proceedings of the 28th European PV Solar Energy Conference and Exhibition, Villepinte, France, 30 September–4 October 2013; pp. 988–992. [CrossRef]

48. Battaglia, C.; De Nicolas, S.M.; De Wolf, S.; Yin, X.; Zheng, M.; Ballif, C.; Javey, A. Silicon heterojunction solar cell with passivated hole selective MoOx contact. *Appl. Phys. Lett.* **2014**, *104*, 113902. [[CrossRef](#)]
49. Kiaee, Z.; Fellmeth, T.; Steinhäuser, B.; Reichel, C.; Nazarzadeh, M.; Nölken, A.C.; Keding, R. TOPCon Silicon Solar Cells with Selectively Doped PECVD Layers Realized by Inkjet-Printing of Phosphorus Dopant Sources. *IEEE J. Photovolt.* **2021**, *13*, 31–37. [[CrossRef](#)]
50. Feldmann, F.; Simon, M.; Bivour, M.; Reichel, C.; Hermle, M.; Glunz, S.W. Efficient carrier-selective p-and n-contacts for Si solar cells. *Sol. Energy Mater. Sol. Cells* **2014**, *131*, 100–104. [[CrossRef](#)]
51. Chen, D.; Chen, Y.; Wang, Z.; Gong, J.; Liu, C.; Zou, Y.; He, Y.; Wang, Y.; Yuan, L.; Lin, W.; et al. 24.58% total area efficiency of screen-printed, large area industrial silicon solar cells with the tunnel oxide passivated contacts (i-TOPCon) design. *Sol. Energy Mater. Sol. Cells* **2020**, *206*, 110258. [[CrossRef](#)]
52. Bullock, J.; Cuevas, A.; Allen, T.; Battaglia, C. Molybdenum oxide MoOx: A versatile hole contact for silicon solar cells. *Appl. Phys. Lett.* **2014**, *105*, 232109. [[CrossRef](#)]

**Disclaimer/Publisher’s Note:** The statements, opinions and data contained in all publications are solely those of the individual author(s) and contributor(s) and not of MDPI and/or the editor(s). MDPI and/or the editor(s) disclaim responsibility for any injury to people or property resulting from any ideas, methods, instructions or products referred to in the content.